Holzforschung, Vol. 62, pp. 737–744, 2008 • Copyright © by Walter de Gruyter • Berlin • New York. DOI 10.1515/HF.2008.115

Impedance spectroscopy and circuit modeling of Southern pine above 20% moisture content

Samuel L. Zelinka[1,]*, Douglas R. Rammer[1] and Donald S. Stone[2]

[1] USDA Forest Service, Forest Products Laboratory, Madison, WI, USA

[2] Department of Materials Science, University of Wisconsin, Madison, WI, USA

*Corresponding author.
USDA Forest Service, Forest Products Laboratory, One Gifford Pinchot Drive, Madison, WI 53726, USA
E-mail: szelinka@fs.fed.us

Abstract

Impedance spectra were collected from Southern pine (*Pinus spp.*) equilibrated to a moisture content 20% and a saturated condition. Cylindrical graphite electrodes were embedded in the wood so that they met nearly end-to-end along a line parallel to the grain, and impedance properties were characterized as functions of electrode spacing and electrode contact pressure at frequencies between 1×10^{-1} and 3×10^{5} Hz. The data exhibit a low-frequency tail that can be fit with a Warburg element, indicative of a diffusive motion of charge carriers. Values of the Warburg impedance were compared with previously published data on molar conductivities of endogenous mineral ions in wood. The data suggest that mineral ions are the predominant charge carriers in wood at low frequencies and high moisture contents based on the strong correlation between the Warburg impedance and molar conductivities.

Keywords: constant phase element; electrical relaxation; electrochemical impedance spectroscopy (EIS); ionic conduction; Warburg impedance.

Introduction

Electrochemical impedance spectroscopy (EIS) has shown promise in its ability to rapidly evaluate the corrosion of metals in contact with wood (Jack and Smedley 1987; Zelinka and Rammer 2005). The major advantage of EIS over other test methods is that it allows modeling the corrosion reaction with an equivalent circuit model. This model, once it has been fit to the data, can then be used as a basis for extrapolating the data to the conditions of interest (MacDonald and Johnson 1987). Equivalent circuit models treat the material system as a collection of electrical components, such as resistors and capacitors, so that the collection replicates the frequency response of the real system. The key of equivalent circuit modeling is that the behaviors represented by the components in the model can be understood in terms of physical mechanisms.

Jack and Smedley (1987) and Zelinka and Rammer (2005) published data of EIS corrosion experiments in wood but did not offer a physical interpretation of the reactions. The reason for this is the information concerning corrosion reaction on the surface of the metal is convoluted with information about the electrical properties of wood does not permit the separation of these convoluted data. Before EIS can be a viable technique for studying corrosion of metals in wood, a thorough understanding of the electrical properties of wood and wood-metal interfaces is needed.

The present EIS measurements are part of a larger, systematic exploration of the electrical properties of Southern pine (*Pinus spp.*) for a better understanding of corrosion tests. The first paper in this series measured the electrical properties at 12% moisture content (MC) (Zelinka et al. 2007). That work showed that electrical properties at frequencies between 1×10^{-1} and 3×10^{5} Hz can be fit using a constant phase element (CPE) in parallel with a resistor (Figures 1 and 2), which corresponds, physically, to a single relaxation mechanism with a narrow distribution of relaxation times. The resistor R_2 represents the direct current (DC) resistivity of the specimen. In some cases, a second resistor (R_1) is needed to describe an additional interfacial resistance. However, we have shown (Zelinka et al. 2007) that this interfacial resistance is negligible for this electrode arrangement. The mean relaxation time, τ_0, was found to be sensitive to contact pressure. It was proposed that this effect might be caused by the effect of pressure on the partitioning of water among different physical or chemical sites within the cell walls, although at that time the mechanism of the relaxation was not clear.

Here, we report on measurements and equivalent circuit modeling of wood at 20% MC and a saturated condition. One of the aims of this work was to identify whether trends seen at 12% MC extend to higher MCs and if information from the higher MC provides additional insight into the physical mechanism(s) of electrical conduction in wood. The mechanism of conduction will be discussed and data of EIS measured conductivities will be compared with literature data.

Material and methods

Half the specimens were prepared by storing the wood at 27°C and 90% relative humidity (RH), which corresponds to a nominal MC of 20% (Forest Products Laboratory 1999) and were tested in the same environment. The other specimens were saturated by placing them in a pressure vessel, drawing a vacuum for 30 min, allowing distilled water to enter into the vessel so that it completely covered the specimens, and then pressurizing the

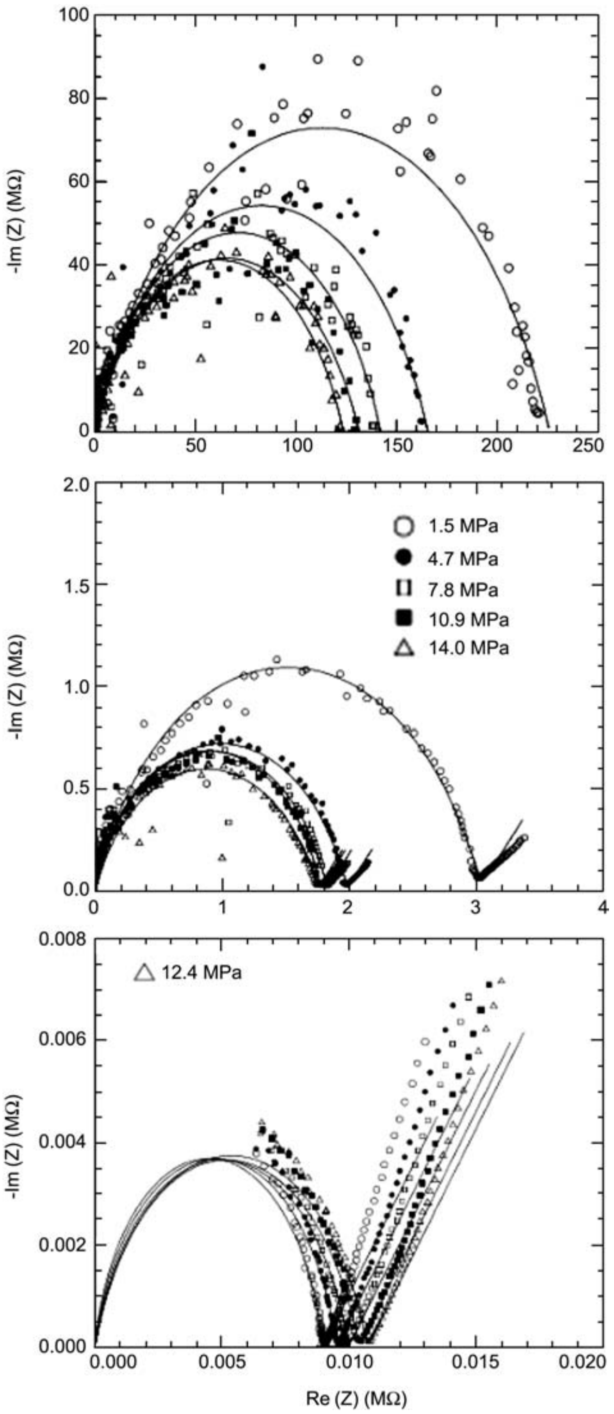

Figure 1 Representative impedance spectra with an electrode spacing of 6.4 mm at 12% MC (top), 20% MC (middle), and at the saturated condition (bottom). Solid lines represent the equivalent circuit model fit. Note the difference in scale between subfigures. MC = moisture content.

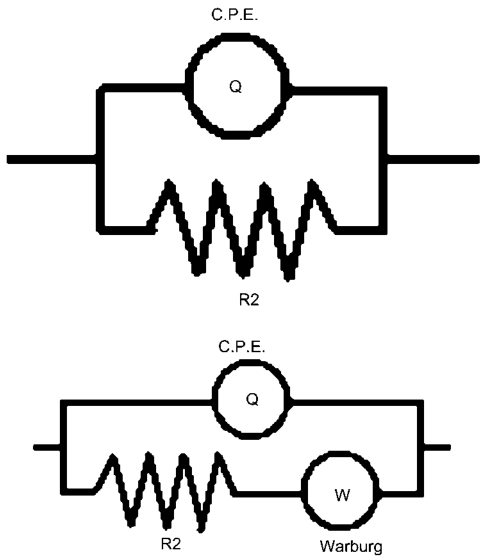

Figure 2 (Top) Two-parameter CPE model used to describe the electrical properties of wood at 12% MC (Zelinka et al. 2007). (Bottom) Equivalent circuit model for the 20% MC and the saturated data. MC = moisture content.

Table 1 Actual moisture content of all specimens tested.

Electrode spacing (mm)	Actual moisture content (%)	
	Nominal 20% MC	Saturated MC
3.2	18.5	149
6.4	18.5	151
12.7	19.4	153
19.0	19.4	145
25.4	19.5	152

vessel at 1.0 MPa for 60 min; tests were run at room temperature in a chamber with a high RH to minimize drying during testing. The mass of each specimen was measured both before and after testing. Actual MCs for all specimens tested are presented in Table 1; for saturated specimens, the reported MC is the average of pre- and post-test MC measurements.

Five specimens were machined for each MC, each specimen with a different electrode spacing (3.2, 6.4, 12.7, 19.0, and 25.4 mm). Nine pressures were applied incrementally to each of the five specimens (1.6, 3.1, 4.7, 6.2, 7.8, 9.3, 10.9, 12.4, and 14.0 MPa). Preliminary results showed no hysteresis with pressure. In some cases, pressure caused the graphite electrodes to buckle. Due to electrode buckling, spectra were not collected for the following conditions: 1) 20% MC, 3.2 mm, 14.0 MPa; 2) saturated condition, all spacings, 14.0 MPa; and 3) saturated condition, 25.4 mm, 9.3–14.0 MPa.

Cylindrical graphite electrodes were embedded in the wood so that they met nearly end-to-end along a line parallel to the grain. The root mean square amplitude of the applied voltage was 10 mV, and the range of frequencies tested was 3×10^5 Hz to 1×10^{-1} Hz. In total, 20 discrete frequencies, spaced logarithmically, were measured for every decade of frequency for a total of 131 measurements per spectrum. All measurements were taken at 0 V with respect to the open circuit potential by connecting the lead for the reference electrode to the counter electrode. This method circumvented the need for a reference electrode (Mansfeld 2003). Further experimental details and a figure of the experimental setup can be found elsewhere (Zelinka et al. 2007).

Results

20% Moisture content

In all, 44 impedance spectra were collected at the 20% MC condition. Figure 1 (middle) shows a representative family of curves with an electrode spacing of 6.4 mm (0.25 in.), in which the frequency, ω, is contained implicitly. Spectra taken at other electrode spacings are qualitatively similar; quantitative data are presented from other spacings in Figures 4–6. Visual comparison of the

20% MC data with those taken at 12% MC (Figure 1) reveals several key differences in the spectra.

First, both -Im(Z) and Re(Z) in the 20% MC samples are approximately a factor of 100 lower than their 12% MC counterparts. This is hardly surprising because it is well documented that the electrical properties of wood are strongly influenced by its MC (Brown et al. 1963; Lin 1965; Skaar 1988). Our data agree with previously published data on slash pine (*Pinus ellioti*) at various MCs (Stamm 1964) (Figure 3).

Second, the 20% MC data appear less noisy than those taken at 12% MC, which is probably related to the fact that the impedances of the latter were on the limits of detection by the equipment (O'Hayre et al. 2004).

Third, the 20% MC data contain a linear region at low frequencies, which is indicative of a diffusive type process (MacDonald and Johnson 1987; Raistrick et al. 1987).

Mathematically, both the high-frequency semicircle and low-frequency tail in Figure 1 can be accounted for by taking the CPE model and adding a Warburg element in series with the resistor to account for the low-frequency behavior (Figure 2). The model presented in Figure 2 (bottom) is a standard one often used in the literature to describe reactions partially controlled by diffusion (Dobbelaar 1963; MacDonald and Johnson 1987; Mansfeld et al. 1993; Jones 1996). The Warburg impedance has the form:

$$Z=\frac{\sigma_w}{\sqrt{\omega}}(1-\hat{j}) \qquad (1)$$

where ω is the angular frequency, $\hat{j}=\sqrt{-1}$, and σ_w is the Warburg coefficient. The fits of the model in Figure 2 (bottom) to experimental data are presented as overlays in Figure 1 (middle).

Saturated condition

In all, 37 impedance spectra were collected at the saturated condition. Figure 1 (bottom) displays a representative family of curves with an electrode spacing of 6.4 mm (0.25 in.). As with the 20% MC data, spectra taken at other electrode spacings are qualitatively similar; quantitative data are presented from other spacings in Figures 4–6. At first glance, the spectra for the saturated samples appear very different from their 12% and 20% MC counterparts; nevertheless, the saturated data can actually be fit quite well with the same model that is used for 20% MC (Figure 2, bottom). The reason that the data appear different is that τ_0 has decreased significantly from the 20% MC case, and now only a portion of the characteristic semi-circle appears in the frequencies tested.

The saturated data differ in another way from their lower MC counterparts (Figure 1). In the latter case, pressure increment decreases the magnitude of both -Im(Z) and Re(Z) at a given frequency. For the saturated data this behavior is reversed.

Finally, it should be noted that the resistivity, calculated from the R_2 parameter of the model, agrees closely with previously measured resistivity data measured in pine (Figure 3).

Discussion

The equivalent circuit model shown in Figure 2 (bottom) can be used to describe data from both the 20% MC and the saturated conditions. The model contains three essential parameters: the mean time constant, τ_0, the

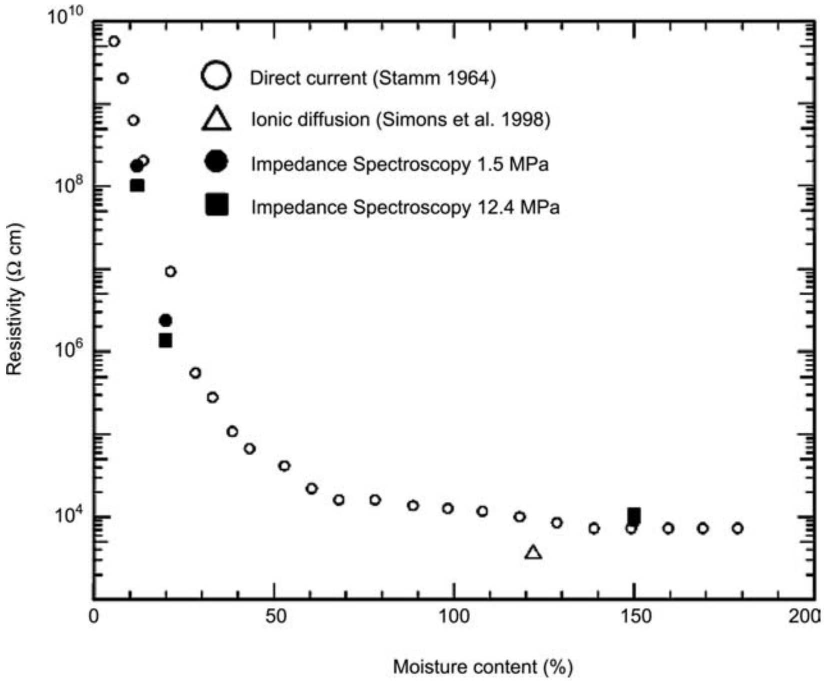

Figure 3 Resistivity as a function of moisture content from Stamm (1964) (*Pinus ellioti*), Simons et al. (1998b) (*Pinus sylvestris*), and in this study at two contact pressures.

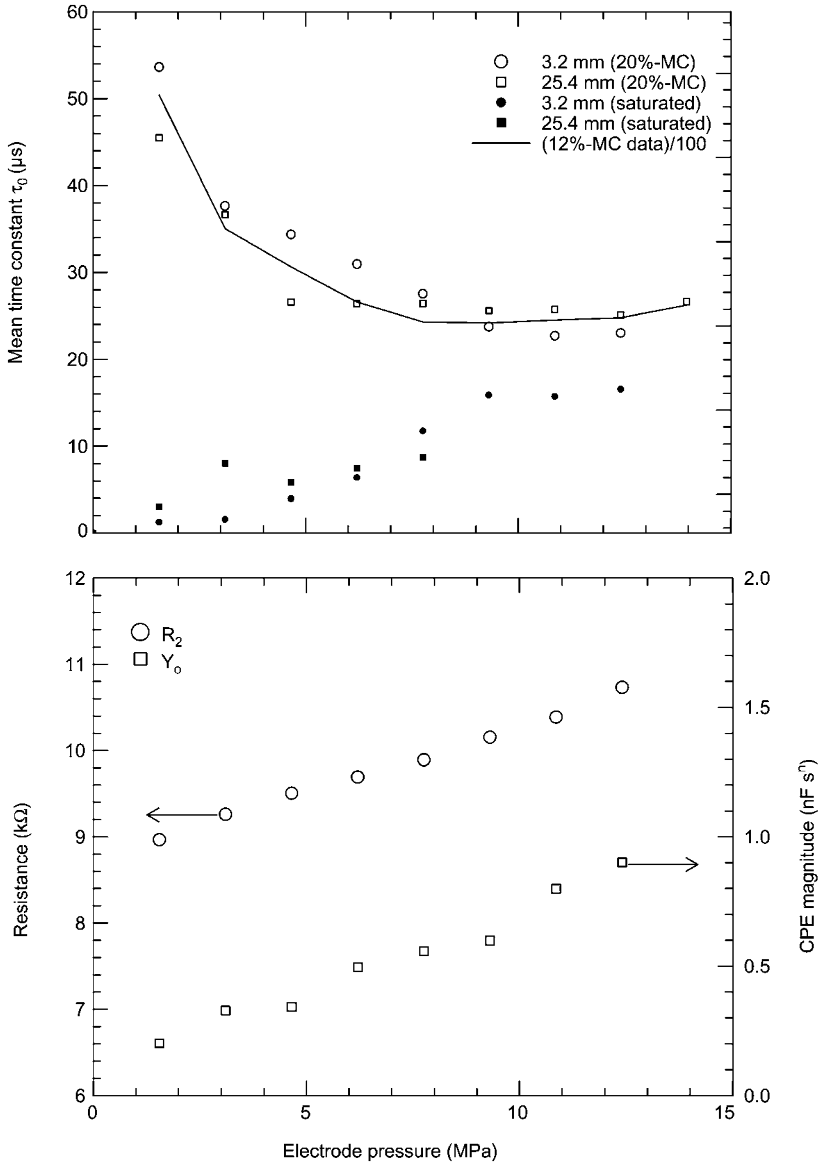

Figure 4 (Top) Mean time constant, τ_0, as a function of pressure. The 12% MC data (divided by 100) from the 3.2-mm spacing are also shown to illustrate the similarities to the 20% MC data. Data for the conditions not shown followed the same general trends and can be found elsewhere (Zelinka 2006). (Bottom) R_2 and Y_0 as functions of electrode pressure for the saturated condition. Both R_2 and Y_0 exhibit linearly increasing dependence on pressure, which was not exhibited below FSP.

width of the distribution, w, and the Warburg coefficient, σ_w. Two of these parameters, τ_0 and w, are associated with the high-frequency "semi-circle", whereas the third parameter, σ_w, represents the low-frequency linear "tail" associated with long-range diffusion of ions.

The mean time constant represents the time required for the material to change its polarization in response to the switching of an electric field. In terms of circuit parameters, this time constant is given by:

$$\tau_0=(R_2Y_0)^{1/n} \tag{2}$$

where R_2 represents the resistor, Y_0 the magnitude of the CPE, and n the exponent associated with the CPE (Cole and Cole 1941; Raistrick et al. 1987). The width of the distribution, defined as the full width at half the maximum value on a $\log_e$ scale, is given by Cole and Cole (1941) as:

$$w=\frac{2\cosh^{-1}\{2-\cos[(1-n)\pi]\}}{n} \tag{3}$$

Several authors have stated that the Warburg impedance corresponds physically to diffusion transport across an infinite media (Dobbelaar 1963; MacDonald and Johnson 1987; Mansfeld et al. 1993; Jones 1996). The Warburg coefficient, σ_w, can be related to the diffusion constants and concentration of the charge carriers by:

$$\sigma_w=\frac{RT}{z_i^2F^2A\sqrt{2}}\sum_i\left|\frac{1}{c_i\sqrt{D_i}}\right| \tag{4}$$

where R is the gas constant (8.314 J mol^{-1} K^{-1}), T absolute temperature, z_i the valence of the ith ionic species, F Faraday's constant (96 500 C mol^{-1}), A the area of the electrode, c_i the concentration of the ith ionic species,

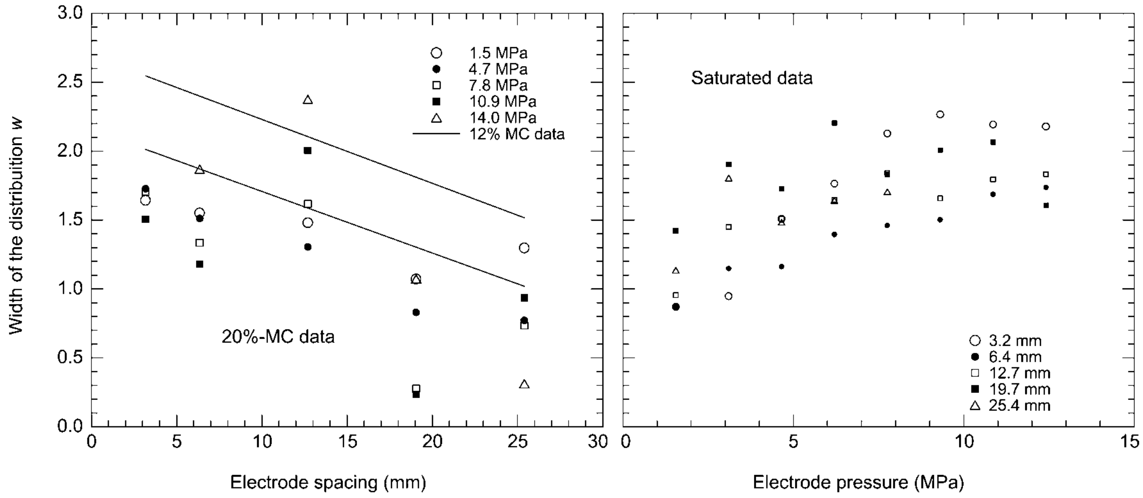

Figure 5 (Left) Width of the distribution, *w*, as a function of electrode spacing for data collected at 20% MC. Solid lines represent maximum and minimum bounds collected at 12% MC. (Right) Width of the distribution as a function of pressure for the saturated condition. Data for the conditions not shown followed the same general trends and can be found elsewhere (Zelinka 2006).

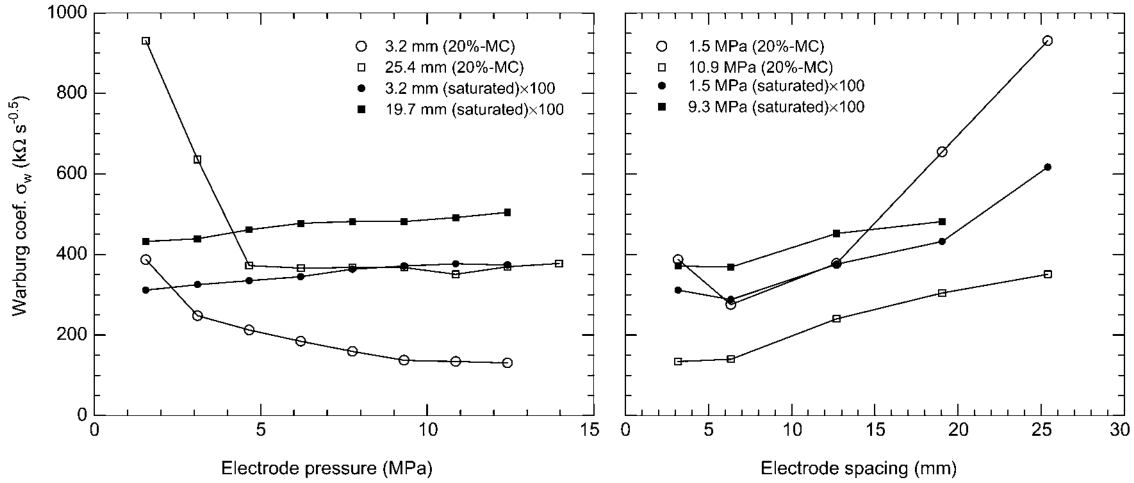

Figure 6 Warburg coefficient as a function of electrode pressure (left) and electrode spacing (right) for both conditions tested. The saturated data (filled symbols) were multiplied by 100 so that they could be plotted on the same axis as the 20% MC data. Data for the conditions not shown followed the same general trends and can be found elsewhere (Zelinka 2006).

and D_i the diffusion constant of the *i*th ionic species (MacDonald and Johnson 1987; Raistrick et al. 1987).

For the 20% MC spectra, τ_0 and *w* behave much the same as they did for the 12% MC wood, except that τ_0 is greatly reduced at 20% MC. The Warburg element was not seen in the 12% MC data, an indication that either the mechanism is absent or the kinetics associated with it are so slow that they cannot be detected without going to lower frequencies. Below, we argue that the former explanation is more likely the correct one and that there is a threshold MC below which long-range diffusion of ions simply does not take place.

The data collected at the saturated condition can be described by the same equivalent circuit model as the 20% MC data. However, at this saturated condition, the independent variables cause τ_0, *w*, and σ_w to behave differently than they did at 12% and 20% MC. This change in behavior is most likely due to the different configuration of water within the wood above the fiber saturation point (FSP), where free water collects in the lumens.

Below, we examine the behavior of τ_0, *w*, and σ_w for both the 20% MC condition and the saturated condition.

Mean time constant

For the 20% MC data (Figure 4), τ_0 generally decreases, then saturates with increasing contact pressure, but it shows no significant trend as a function of electrode spacing; the mean time constant is relatively insensitive to spacing, which was interpreted previously that τ_0 is an intensive material parameter.

For the saturated condition, the mean time constant is a little more than 10 times smaller than it is for the 20% MC condition (Figure 4). Again, as in the 12% MC case, we observe that the mean time constant is independent of electrode spacing. For the 12% MC data, we demonstrated that this independence implies that the resistance and capacitance of the wood-electrode interface are negligible. This independence at higher MC means that interfacial effects remain negligible even above FSP.

In contrast to the 20% MC data, where τ_0 decreases with pressure to approach an asymptote at high pressures, in the saturated wood, τ_0 increases approximately linearly with increasing contact pressure. Previously, for readings at 12% MC (Zelinka et al. 2007), it was proposed that pressure causes τ_0 to change by altering the partitioning of water among the various chemically and physically distinct sites within the cell wall. The high-pressure asymptote occurs in the 12% MC data, because a saturation in τ_0 is reached as the type of site favored at high pressures becomes fully populated. This asymptotic behavior is again observed in the 20% MC data but not in the data collected at the saturated condition (Figure 4). Although the data taken from saturated samples have a completely different behavior, they are not inconsistent with this picture; above FSP, increasing pressure will not likely change the partitioning of water within the cell wall, because all the different types of sites are filled.

Expanding upon the observed behavior for the saturated condition, τ_0 is a function of both R_2 and Y_0 [Eq. (2)], and the behavior of τ_0 can be expressed in terms of the behavior of R_2 and Y_0 (Figure 4, bottom). For the data taken below FSP, Y_0 remains constant with pressure, while R_2 decreases asymptotically, driving the change in τ_0. However, for the data above FSP, both Y_0 and R_2 increase with pressure. Increasing the electrode pressure above FSP may force some of the water out of the lumens near the electrodes, where pressure is the highest, causing changes in both resistance and capacitance.

Width of the distribution

As with the mean time constant, τ_0, the width of the distribution, *w*, also exhibits large changes between the two MCs examined.

For the 20% MC data, *w* shows no distinct trend with contact pressure but decreases with increasing electrode spacing (Figure 5), much as it did for the 12% MC data. However, for data taken at the saturated condition, *w* increases nearly linearly with electrode pressure but exhibits no dependence on electrode spacing (Figure 5).

In the context of the 12% MC data, it is unclear why the width of the distribution, *w*, decreases linearly with increasing electrode spacing and did not depend on pressure. However, because *w* behaves in a drastically different manner above FSP, the width of the distribution must also be related to the manner in which water is partitioned within the wood.

Warburg impedance

As stated earlier, the Warburg impedance can be interpreted in terms of ions diffusing in an infinite media. This behavior was observed in measurements taken at 20% MC and at saturated condition but not in the case of 12% MC. This could be explained by a threshold MC for diffusion as demonstrated by Lin (1965). This author studied the movement of radioactive Na-22 and I-131 ions through western white pine (*Pinus monticola*) at MCs between 5% and 28% in the presence of an electric field and found that long-range movement of ions did not occur at MCs less than 16%. Therefore, the absence of Warburg behavior at 12% MC is consistent with the data of Lin (1965).

For the 20% MC data, σ_w decreases with increasing contact pressure but approaches a high-pressure asymptote at pressures above 5 MPa (Figure 6), which is similar to the behavior of τ_0 at 12% MC. Unlike τ_0, σ_w does depend on electrode spacing (Figure 6). As can be seen in Figure 1, the model does not fit low-frequency data perfectly. Ideally, the slope in the complex plane should be unity [Eq. (1)]; however, in all cases, the slope was slightly less than one.

For the saturated data, σ_w behaves the same way that τ_0 does above fiber saturation, slightly increasing linearly with pressure (Figure 6), just as σ_w and τ_0 exhibit parallel behavior for the 20% MC case. In addition, σ_w increases with increasing electrode spacing as it did for the 20% MC case (Figure 6).

Although it is not universally accepted (Venkateswaran 1974; Hou et al. 2004), the majority of researchers have written compelling arguments that in the DC limit, the charge is carried by endogenous mineral ions, such as potassium, sodium, calcium, and magnesium (Langwig and Meyer 1973; Simons et al. 1998a,b). Therefore, we should be able to relate the diffusion coefficients of endogenous mineral ions to the Warburg coefficient, σ_w.

Simons et al. (1998b) published DC molar conductivities for several different ions in Scots pine (*Pinus sylvestris*) at 120% MC. The molar conductivity of ionic species *i*, λ_i, can be related to the diffusion coefficient, D_i, through:

$$D_i=\left(\frac{RT}{F^2}\right)\left(\frac{\lambda_i}{|z_i|}\right) \tag{5}$$

where *R, T, F,* and *z* have the same definitions as in Eq. (4) (Vanysek 2005). These diffusion coefficients can then be used in Eq. (4) to calculate the Warburg coefficient.

Table 2 contains published values (Simons et al. 1998b) of the molar conductivity and concentration of endogenous mineral ions in Scots pine at 120% MC, along with calculated diffusion coefficients and the resulting Warburg coefficient. The Warburg coefficient of Simons et al. (1998b) can be expected being lower in magnitude than that taken at 20% MC, because the diffusion coefficients increase with increasing MC and σ_w is inversely proportional to $\sqrt{D_i}$.

Table 2 Molar conductivities and concentrations of endogenous mineral ions[a] and calculated diffusion and Warburg coefficients.

	λ_i (cm^2 Ω^{-1} mol^{-1})	c_i (mol cm^{-3})	D_i (cm^2 s^{-1})	σ_w (Ω s$^{-0.5}$)
K^+	8.7	5.45×10^{-6}	2.33×10^{-6}	18
Na^+	9.2	4.30×10^{-7}	2.47×10^{-6}	222
Ca^{2+}	3.8	6.17×10^{-6}	5.09×10^{-7}	8
Mg^{2+}	1.3	2.58×10^{-6}	1.74×10^{-7}	34
Cl^-	14.6	4.30×10^{-7}	3.91×10^{-6}	176
Total				458

[a]From Simons et al. (1998b).

The calculated Warburg coefficient for Scots pine at 120% MC is approximately 450 Ω $s^{-0.5}$, which is smaller by a factor of 1.5×10^{-3} than the empirically fit Warburg coefficient we found for Southern pine at 20% MC (Figure 6), whose mean value is 3.01×10^{5} Ω $s^{-0.5}$. Given the lower MC of the current experiment, this ratio is what can be expected by assuming that the magnitude of the Warburg impedance scales with resistivity (Figure 3). The ratio of the resistivity reported by Simons et al. (1998b) for Southern pine at 120% MC fits to the resistivity measured at 1.5 MPa pressure in this study is 1.6×10^{-3}.

The magnitude of the Warburg impedance for the saturated specimens at 150% MC ($\sim$4000 Ω $s^{-0.5}$) is approximately 100 times less than the impedance found at 20% MC but is still almost 10 times greater than that found by Simons et al. (1998b). However, Simons et al. (1998b) also measured a lower resistivity than was measured in this study and used a different technique to measure ionic diffusivity. Differences between these two results are most likely caused by differences in experimental techniques. Given this correlation, the Warburg impedance applied in this model likely represents the diffusive motion of endogenous mineral ions through the wood.

Note that ionic conduction, which in the wood literature is usually thought of as an aqueous process (Brown et al. 1963), has a threshold between 15% and 20% MC, well below the traditional fiber saturation point, at which water fills the lumens. Many other changes that are thought to require free water, such as corrosion in wood (Baker 1987; Dennis et al. 1995) and mold growth on wood (Viitanen 1996), also have a threshold between 15% and 20% MC. Therefore, it seems plausible that some loosely bound water is present below FSP, although it remains unclear where it resides. One possibility is that it exists in so-called microcapillaries within the cell wall, which have a diameter of a several nanometers (Wallström and Lindberg 2000). These microcapillaries would be ideal spots for loosely bound water to form, because capillary pressure here would be high and water would therefore condense at a much lower humidity (Skaar 1988).

Conclusions

The electrical properties of Southern pine at two different MCs parallel to the grain were characterized by electrical impedance spectroscopy. In the range of frequencies tested, 1×10^{-1} to 3×10^{5} Hz, the data exhibited a high-frequency relaxation mechanism and a low-frequency diffusive type mechanism. The data were fit with a model similar to that used to model the electrical properties of wood at 12% MC, except that a Warburg element was added to account for what appears to be a diffusion "tail". The Warburg coefficient, σ_w, was related to ionic diffusivity data published by Simons et al. (1998b) on the molar conductivities of endogenous mineral ions in Scots pine (*Pinus sylvestris*) at 120% MC.

The data suggest that electrical properties of wood, at least at low frequencies, most likely result from the diffusive motion of endogenous mineral ions through the wood.

References

Baker, A.J. (1987) Corrosion of metals in preservative-treated wood. In: Wood Protection Techniques and the Use of Treated Wood in Construction. Eds. Hamel, K. Proceedings 47358. Forest Products Research Society, Madison, WI. pp. 99–101.

Brown, J.H., Davidson, R.W., Skaar, C. (1963) Mechanism of electrical conduction in wood. Forest Prod. J. 13:455–459.

Cole, K.S., Cole, R.H. (1941) Dispersion and absorption in dielectrics I. Alternating current characteristics. J. Chem. Phys. 9:341–351.

Dennis, J.K., Zou, C., Short, N.R. (1995) Corrosion behaviour of zinc and zinc alloy coated steel in preservative treated timber. Trans. Inst. Metal Finishing 75:96–101.

Dobbelaar, J.A.L. (1963) The use of impedance measurements in corrosion research: the corrosion behaviour of chromium and iron-chromium alloys. PhD dissertation, Delft University of Technology, Netherlands.

Forest Products Laboratory Wood Handbook – Wood as an Engineering Material. Gen. Tech. Rep. FPL-GTR-113, U.S. Department of Agriculture, Forest Service, Forest Products Laboratory, Madison, WI, 1999.

Hou, Z.Q., Chen, Z., Wright, R.S. (2004) Theoretical exploration of factors affecting dielectric constants of masson pine. Holzforschung 58:418–422.

Jack, E.J., Smedley, S.I. (1987) Electrochemical study of the corrosion of metals in contact with preservative treated wood. Corrosion 43:251–257.

Jones, D.A. Principles and Prevention of Corrosion, 2nd edn. Prentice Hall, Saddle River, NJ, 1996.

Langwig, J.E., Meyer, J.A. (1973) Ion migration in wood verified by neutron activation analysis. Wood Sci. 6:39–50.

Lin, R.T. (1965) A study of electrical conduction in wood. PhD dissertation, State University College of Forestry at Syracuse University Syracuse, New York, USA.

MacDonald, J.R., Johnson, W.B. (1987) Fundamentals of impedance spectroscopy. In: Impedance Spectroscopy Emphasizing Solid Materials and Systems. Ed. MacDonald, J.R. John Wiley & Sons, New York. pp. 1–26.

Mansfeld, F. (2003) Electrochemical methods of corrosion testing. In: ASM Handbook Volume 13A, Corrosion: Fundamentals, Testing, and Protection. Eds. Cramer, S.D., Covino, B.S. ASM International, Materials Park, Ohio, OH. pp. 446–462.

Mansfeld, F., Shih, H., Greene, H., Tsai, C.H. (1993) Analysis of EIS data for common corrosion processes. In: Electrochemical Impedance: Analysis and Interpretation, ASTM STP 1188. Eds. Scully, J.R., Silverman, D.C., Kendig, M.W. American Society for Testing and Materials, Philadelphia, PA. pp. 37–53.

O'Hayre, R., Lee, M., Prinz, F.B. (2004) Ionic and electronic impedance imaging using atomic force microscopy. J. Appl. Phys. 95:8382–8392.

Raistrick, I.D., MacDonald, J.R., Franceschetti, D.R. (1987) The electrical analogs of physical and chemical processes. In: Impedance Spectroscopy Emphasizing Solid Materials and Systems. Ed. MacDonald, J.R. John Wiley & Sons, New York. pp. 27–84.

Simons, P.J., Spiro, M., Levy, J.F. (1998a) Electrical transport of endogenous mineral ions in green sapwood of *Pinus sylvestris* L. (Scots pine). Wood Sci. Technol. 32:403–410.

Simons, P.J., Spiro, M., Levy, J.F. (1998b) Electrical properties of wood: determination of ionic transference numbers and electroosmotic water flow in *Pinus sylvestris* L. (Scots pine). J. Chem. Soc., Faraday Trans. 94:223–226.

Skaar, C. Wood-Water Relations. Springer-Verlag, New York, 1988.

Stamm, A.J. (1964) Electrical properties. In: Wood and Cellulose Science. Ed. Stamm, A.J. Ronald Press Company, New York. pp. 359–385.

Vanysek, P. (2005) Ionic conductivity and diffusion at infinite diffusion. In: CRC Handbook of Chemistry and Physics, 85th edn. Ed. Lide, D.R. Chemical Rubber Publishing Company, Boca Raton, FL. pp. 207–262.

Venkateswaran, #. (1974) The interdependence of the lignin content and the electrical properties of wood. Wood Fiber 6:46–52.

Viitanen, H.A. (1996) Factors affecting the development of mould and brown rot decay in wooden material and wooden structures – effect of humidity, temperature and exposure time. PhD dissertation, Swedish University of Agricultural Sciences, Department of Forest Products, Uppsala, Sweden.

Wallström, L., Lindberg, K.A.H. (2000) The diffusion, size and location of added silver grains in the cell walls of Swedish pine, *Pinus sylvestris.* Wood Sci. Technol. 34:403–415.

Zelinka, S.L. (2006) Equivalent circuit modeling of Southern pine. Masters thesis, University of Wisconsin-Madison, Materials Science Program, Madison, WI, USA.

Zelinka, S.L., Rammer, D.R. (2005) The use of electrochemical impedance spectroscopy (EIS) to measure the corrosion of metals in contact with wood. TMS Lett. 2:15–16.

Zelinka, S.L., Stone, D.S., Rammer, D.R. (2007) Equivalent circuit modeling of wood at 12% moisture content. Wood Fiber Sci. 39:556–565.

Received March 28, 2008. Accepted July 24, 2008.
Previously published online September 12, 2008.